INSTITUTE OF PHYSICS PUBLISHING JOURNAL OF PHYSICS G: NUCLEAR AND PARTICLE PHYSICS

J. Phys. G: Nucl. Part. Phys. **32** (2006) S61–S68 doi:10.1088/0954-3899/32/12/S07

Recent results from BRAHMS in the context of longitudinal dynamics at RHIC

J H Lee (for the BRAHMS Collaboration[1])

Physics Department, Brookhaven National Laboratory Upton, NY 11973, USA

E-mail: jhlee@bnl.gov

Received 27 July 2006
Published 17 November 2006
Online at stacks.iop.org/JPhysG/32/S61

Abstract
The BRAHMS Collaboration has measured identified charged hadron production as a function of rapidity for Au+Au and Cu+Cu collisions at energies of $\sqrt{s_{NN}} = 200$ and 62.4 GeV at RHIC. Selected recent results are presented with emphasis on longitudinal dynamics of particle production. The rapidity dependence of particle production imposes stringent additional constraints on theoretical models describing dynamics of hadronic/partonic matter created by high-energy heavy-ion collisions.

(Some figures in this article are in colour only in the electronic version)

1. Introduction

The central theme of studying heavy-ion collisions at relativistic energy regime has been to identify matter with partonic degrees of freedom, quark–gluon plasma (QGP) [1]. The partonic QCD phases in the highly excited state of the matter are predicted to be accessible by collisions between two heavy nuclei (Au) at the extreme high energy ($\sqrt{s_{NN}} = 200$ GeV) produced at RHIC/BNL, an order of magnitude higher than previously available energy at SPS. The vast body of the measurements at mid-rapidity in central Au+Au collisions obtained by the four experiments at RHIC for the last five years in conjunction with the available theoretical studies indicates that the matter created by heavy-ion collisions at RHIC cannot be characterized solely by hadronic degrees of freedom. This state with partonic degree of freedom is referred as empirical QGP—'sQGP', strongly coupled QGP [2], not however the weakly interacting, colour-dielectric 'wQGP', that we have searched for.

In order to characterize the nature of the created nuclear (partonic or hadronic) matter, it is imperative to study the particle production in a wide kinematic range (y–p_T) beyond the mid-rapidity region to provide stringent constraints on theoretical interpretations of matter formed in heavy-ion collisions. In particular, the study of the rapidity dependence of particles

[1] A list of members of the BRAHMS Collaboration is given at the end of this issue.

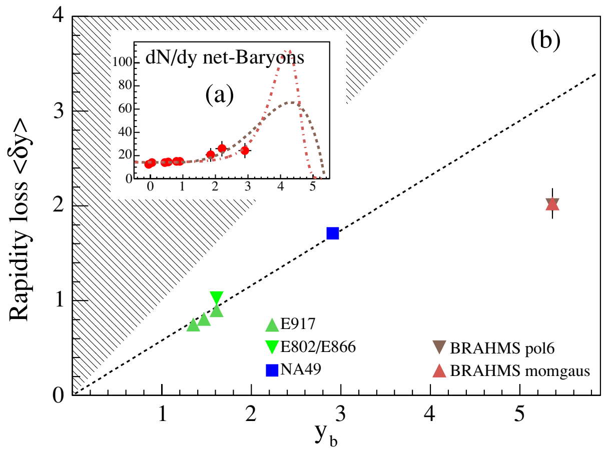

Figure 1. Inset: estimates of net baryon distributions exploiting baryon number conservation. Average rapidity loss as deduced from net proton distribution versus beam rapidity is shown in the main panel. The line is the linear extrapolation from [6].

emitted in heavy-ion collisions addresses the following:

- Baryon stopping and total energy released in the reaction,
- Longitudinal flow of matter created,
- Strangeness abundance and quark chemistry,
- Dynamical medium effects and
- Non-perturbative mechanism in the high-p_T regime.

We present selected recent results on rapidity (y) and transverse momentum (p_T)-dependent particle production in Au+Au, Cu+Cu and p+p collisions measured by BRAHMS spectrometers at RHIC in the context of physics listed above. A more extensive summary of BRAHMS results is described in [3]. Details of the BRAHMS experimental set-up can be found in [4].

2. Results

2.1. Energy released from the collisions and limiting fragmentation

Since the number of baryons is conserved in the nuclear collisions, the measured net baryon $(B - \bar{B})$ distribution retains information about the energy loss in the reaction and allows the degree of nuclear stopping to be determined. We have measured the rapidity-dependent net proton $(p - \bar{p})$ distribution in central Au+Au collisions [5]. The net number of protons per unit of rapidity around $y = 0$ is about 7 and the distribution is flat over at least ± 1 unit of rapidity. The distribution increases in the rapidity range $y = 2$–3 to an average $\mathrm{d}N/\mathrm{d}y \approx 12$. Figure 1 (insert) shows $\mathrm{d}N/\mathrm{d}y$ distributions versus y, assuming two different functions (Gaussian in p_L and sixth-order polynomial) with a constraint that integral areas correspond to the number of participant nucleons. A set of upper and lower limits for the rapidity loss can be deduced from the distributions. We assume that $N(n) \approx N(p)$ and scaled Λ yields at mid-rapidity to forward rapidities using HIJING [5]. The rapidity loss is estimated to be $\delta y = 2.05 \pm 0.17$. This estimated loss is less than the phenomenological linear rapidity scaling extrapolated from measurements at lower energies as shown in figure 1. The average energy loss from the

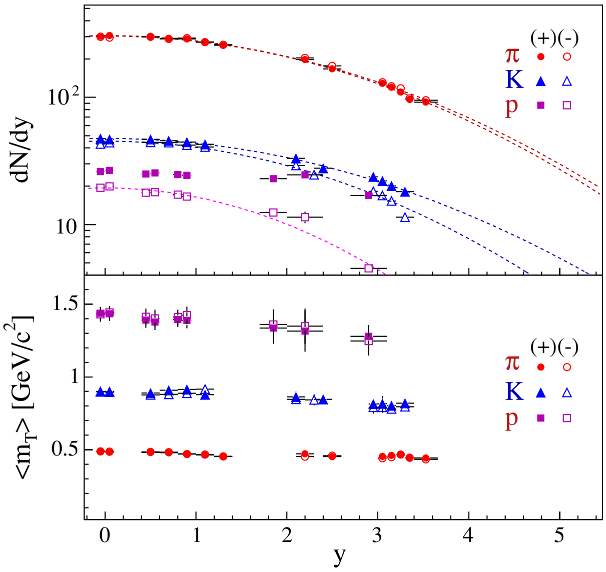

Figure 2. Top: rapidity distribution for positive and negative pions, kaons and protons. The lines show Gaussian fits. Bottom: average m_T values as a function of rapidity.

collisions corresponds to about 73 ± 6 GeV per nucleon during the collision. The rapidity densities of the net proton in p+p collisions at the same energy show a similar distributions [7]. These results are qualitatively consistent with Bjorken's model of the ultra-high-energy nuclear collision where the fragmentation regions are assumed to be near the beam rapidity away from mid-rapidity [8]. It has been known that the particle production in the fragmentation regions near the beam rapidity is essentially independent of the collision energy, a phenomenon known as 'limiting fragmentation' [9]. The scaling has been observed in Au+Au and d+Au collisions by BRAHMS [10, 11] and PHOBOS experiments [12] at RHIC. More extended longitudinal scaling behaviour spanning whole rapidity range, from near beam rapidity to mid-rapidity, is observed for $\langle p_T \rangle$ [13] and elliptic (v_2) and directed (v_1) flow parameters [14, 15]. The degree to which the energy independence of these scaling observations extends to mid-rapidity is intriguing. They imply the longitudinal degree of freedom is not to be treated trivially in experimental and theoretical efforts to understand nuclear collisions at RHIC.

2.2. Particle production and flow

Figure 2 shows rapidity densities of charged pions, kaons and protons for central Au+Au collisions. The particle-to-antiparticle ratio is seen to be approaching unity in an interval of about 1.5 units of rapidity around mid-rapidity, suggesting that the particle production in the central region is predominantly from pair creation. This is true for pions, but less so for kaons ($R_{K^-/K^+} = 0.95$) and protons ($R_{\bar{p}/p} = 0.76$) [16]. The observed pion rapidity distributions exhibit a nearly Gaussian shape. Widths are found to be $\sigma_{\pi^+} = 2.27 \pm 0.02$(stat) and $\sigma_{\pi^-} = 2.31 \pm 0.02$. This is reminiscent of the hydro-dynamical expansion model proposed by Landau [17]. Under assumptions of isentropic expansion, the hydro-dynamical equations, using the equation of state of a relativistic gas of massless particles, lead to $\mathrm{d}N/\mathrm{d}y$ distributions of approximately Gaussian shape at freeze-out [18]. In a simplified version of the Landau model [19–21] developed for the description of particle production in p+p collisions, the width

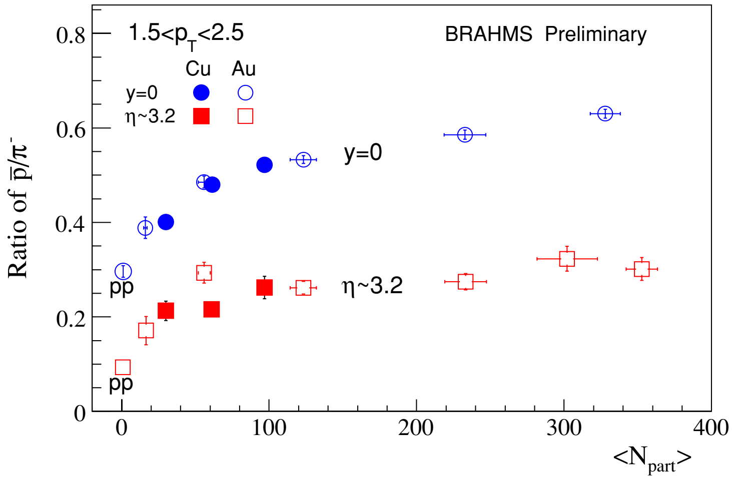

Figure 3. The averaged $\bar{p}/\pi^-$ as a function of $\langle N_{\mathrm{part}}\rangle$ for Au+Au (open symbols) and Cu+Cu (solid symbols) at $\sqrt{s_{NN}} = 200$ GeV, for $y \sim 0$ (circles) and for $\eta \sim 3.2$ (squares).

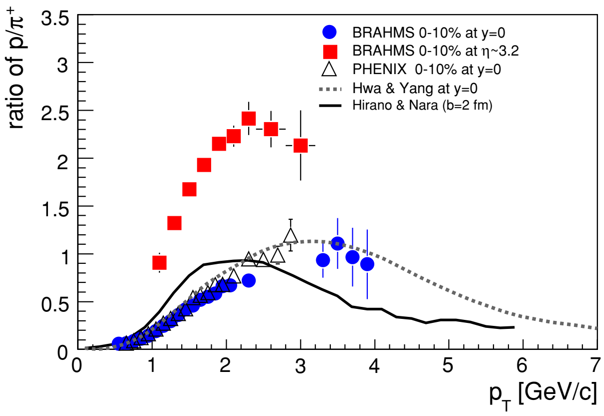

Figure 4. The p/π^+ ratio versus p_T for Au+Au collisions at $\sqrt{s_{NN}} = 200$ GeV measured at mid-rapidity by BRAHMS (circles) and by PHENIX (triangles). Squares represent BRAHMS results at $\eta \sim 3.2$. The plotted lines show theoretical model calculations.

σ of the pion distribution is formulated as $\sigma^2 = \ln\gamma_{\mathrm{beam}} = \ln(\sqrt{s}/2m_p)$, where m_p is the proton mass. The observed discrepancy in width for π^- between the model ($\sigma = 2.16$) and the data is $\sim$5%). The measured $\langle m_T\rangle$, where $m_T = \sqrt{p_T^2 + m^2}$, distributions shown in figure 2 in $0 < y < 3$ indicate the presence of strong radial flow at freeze-out in a wide rapidity range, as estimated by hydrodynamics motivated models [22].

2.3. *Rapidity-dependent baryon-to-meson ratios*

It has been observed that for Au+Au reactions in the intermediate p_T region the p/π^+ and $\bar{p}/\pi^-$ ratios are significantly higher than one would expect from the parton fragmentation in processes in the vacuum. Several theoretical models have been proposed to explain the observed enhancement. These range from models that explore the partonic interactions of

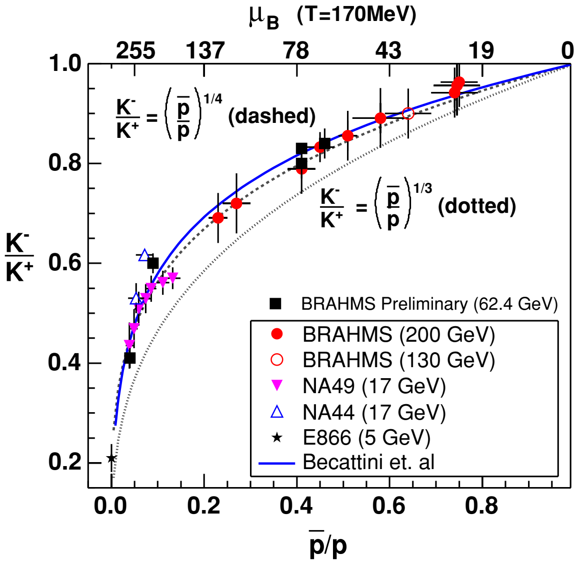

Figure 5. Correlation between K^-/K^+ and $\bar{p}/p$. The BRAHMS measurements are from different rapidities in the range $0 < y < 3$. The solid curve corresponds to a statistical model calculation with chemical freeze-out temperature of 170 MeV. The dashed line ($\alpha = 1/3$) represents a statistical assumption based on chemical and thermal equilibrium at the quark level. The dashed curve is with $\alpha = 1/4$, which follows well the statistical model prediction.

quark hadronization and quark coalescence [23–25] to models that incorporate novel baryon dynamics [26, 27]. Figure 3 shows $\bar{p}/\pi^-$ ratios for $1.5 < p_T < 2.5$ GeV/c at mid-rapidity and at pseudo-rapidity $\eta \sim 3.2$ for Au+Au and Cu+Cu at $\sqrt{s_{NN}} = 200$ GeV. One can see a strong increase of the $\bar{p}/\pi^-$ ratio as a function of $\langle N_{\text{part}}\rangle$ in the range $N_{\text{part}} \leqslant 60$ and the dependence starts to saturate and the ratios reach values of about ~ 0.6 and about 0.25 for central collisions at mid- and forward rapidities, respectively. For peripheral Au+Au collisions the data approach the p+p results. Figure 4 shows a comparison of BRAHMS and PHENIX [28] data for the ratio of protons to π^+ measured at $y = 0$. The parton coalescence [24] and recombination [25] models describe the observed ratios well at mid-rapidity. The three-dimensional hydrodynamical calculations [29] do not show a rapidity dependence which is in contrast to the experimental observation. This is presumably because the hydrodynamic models do not assume a rapidity-dependent baryo-chemical potential.

2.4. Strangeness abundance and quark chemistry

Figure 5 shows the N_{K^-}/N_{K^+} ratios as a function of the corresponding $N_{\bar{p}}/N_p$ for various rapidities ($0 < y < 3$) in central Au+Au collisions at RHIC. The figure also displays similar ratios for heavy-ion collisions at AGS and SPS energies. The N_{K^-}/N_{K^+} and $N_{\bar{p}}/N_p$ ratios increase as rapidity increases. This is consistent with an increase of net baryon densities. A baryon-rich environment is favourable for associated strangeness production, e.g. $p + p \to p + K^+ + \Lambda$, a production channel forbidden for K^-.

There is a strong correlation between the RHIC/BRAHMS kaon and proton ratios over three units of rapidity. It is worth noting that the BRAHMS forward rapidity data measured at $\sqrt{s_{NN}} = 62.4$ GeV overlap with the SPS points that were measured at much lower energy

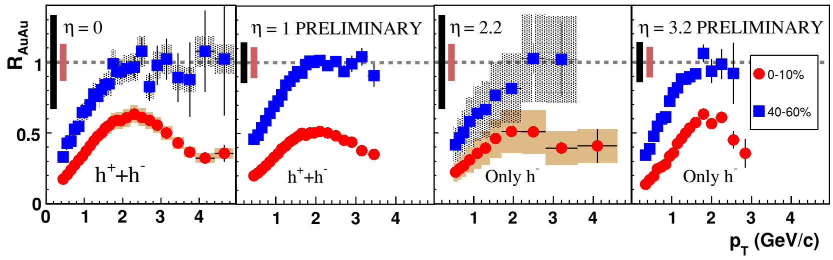

Figure 6. Nuclear modification factor R_{AuAu} for charged hadrons measured at $\eta = 0$, 1, 2.2, and 3.2 for 0–10% (circle) and 40–60% (square) central Au+Au collisions at $\sqrt{s_{NN}}$=200 GeV.

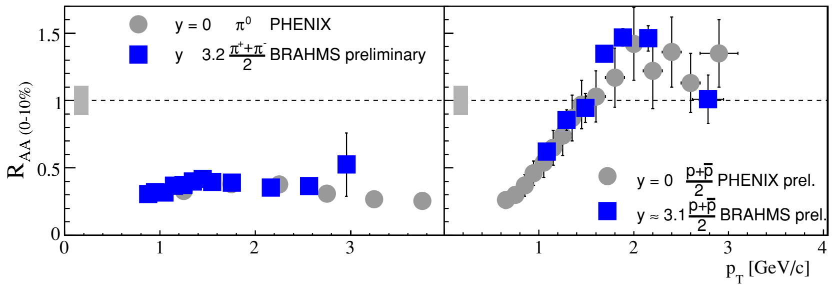

Figure 7. Nuclear modification factor R_{AuAu} for charged hadrons measured at $y = 0$ (circle) and $y \sim 3$ (square) for 0–10% central Au+Au collisions for pions and protons at $\sqrt{s_{NN}} = 200$ GeV.

but at mid-rapidity. It is seen that the data are very well described by the statistical model [30] over a broad rapidity range with the baryon chemical potential changing from 27 MeV at mid-rapidity to 140 MeV at the most forward rapidities. This may be an indication that the system is in (local) chemical equilibrium over the considered $\sqrt{s}$ and y ranges.

2.5. *Rapidity-dependent high-p_T suppression: studying dynamical medium effect*

Jet quenching, i.e. non-Abelian radiative energy loss due to multiple gluon emission off the hard scattered partons in dense QCD matter, has been used as an important probe for dense matter. Hadron spectra at high p_T in central Au+Au collisions at mid-rapidity are strongly suppressed relative to spectra from pp or peripheral collisions scaled by the number of binary collisions. That is consistent with the description of jet quenching in medium with high energy density created by the collisions. Because jet energy loss is expected to be proportional to the density of the local medium, at different rapidities the leading high-p_T hadron from jet fragmentation will also show different behaviour. Thus studying nuclear modification beyond mid-rapidity can provide a novel way to study how dense matter is distributed in the longitudinal direction.

BRAHMS has reported the pseudo-rapidity (η) dependence of the nuclear modification factors and showed that the yields of high-p_T charged hadrons are strongly suppressed even at $\eta \sim 2.2$ [31]. The preliminary results shown in figure 6 indicate that at higher rapidities the suppression persists to a similar degree as at $y \sim 0$. Figure 7 shows the identified particle nuclear modification factors for $(\pi^+ + \pi^-)/2$ and $(\bar{p} + p)/2$ at $y \sim 3.2$, and compared with measurements from PHENIX for central Au+Au collisions. The nuclear modification factors show very similar behaviour at $y \sim 0$ and $y \sim 3.2$. The suppression is reduced at 62.4 GeV at

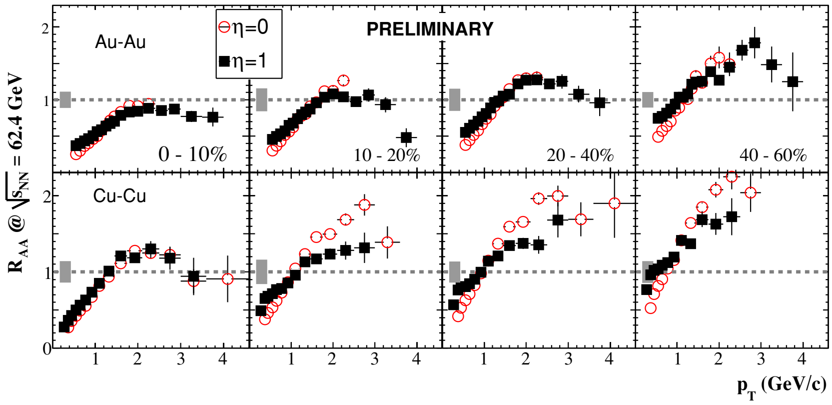

Figure 8. Centrality dependent R_{AA} for charged hadrons measured at $\eta = 0$ and 1 for Au+Au (upper row) and for Cu+Cu (bottom row) at $\sqrt{s_{NN}} = 62.4$ GeV.

near mid-rapidity for Au+Au and even more reduced for Cu+Cu at the same energy indicating that the nuclear modification is strongly dependent on collision energy and system sizes, as shown in figure 8. This indicates that either the high-p_T suppressing medium is substantially extended longitudinally and/or there is some other (non-perturbative) mechanism causing apparent strong nuclear modification [2, 32] at forward rapidities. There have been some theoretical attempts [29, 33] to explain the longitudinal suppression mechanism, but more quantitative theoretical description of the data is needed.

These measurements, in conjunction with measurements of nuclear modification at forward rapidities in d+Au collisions [34], should provide input and constraints for the theoretical modelling of the dynamics of the energy loss due to the high-density medium effect in the context of spacetime evolution of the parton density.

3. Conclusions

The vast body of the measurements at mid-rapidity in central Au+Au collisions obtained by the four experiments at RHIC in conjunction with the available theoretical studies indicates that the matter created by heavy-ion collisions at RHIC cannot be characterized solely by hadronic degrees of freedom. This state with partonic degree of freedom is referred as the strongly coupled QGP. The BRAHMS experiment has been studying the high temperature and density phase of the matter beyond the mid-rapidity exploring longitudinal dynamics of the state. Identifying the properties of the high energy density requires theoretical modelling. No currently available theoretical model successfully reproduces all aspects of the rapidity dependence of particle production. The rapidity dependence results for various systems and at different collision energies will serve as an important link to firmly connect the experimental measurements on the properties of the matter created in the collision with our current theoretical understanding.

Acknowledgment

This work is supported by the Division of Nuclear Physics of the Office of Science of the US Department of Energy under contract DE-AC02-98-CH10886.

References

[1] For a review, see Kapusta J, Müller B and Rafelski J 2003 *Quark–Gluon Plasma: Theoretical Foundations* (Amsterdam: Elsevier) chapter 2
[2] Gyulassy M and McLerran L 2005 *Nucl. Phys.* A **750** 30
[3] BRAHMS Collaboration 2005 *Nucl. Phys.* A **757** 1
[4] BRAHMS Collaboration 2003 *Nucl. Phys.* A **499** 437
[5] BRAHMS Collaboration 2004 *Phys. Rev. Lett.* **93** 102301
[6] Videbaek F and Hansen O 1995 *Phys. Rev.* C **52** 2584
[7] Yang H (BRAHMS Collaboration) 2006 *J. Phys. G: Nucl. Phys.* **32** S491 (these proceedings)
[8] Bjorken J D 1983 *Phys. Rev.* D **27** 140
[9] Benecke J *et al* 1969 *Phys. Rev.* **188** 2159
[10] BRAHMS Collaboration 2002 *Phys. Rev. Lett.* **88** 202301
[11] BRAHMS Collaboration 2005 *Phys. Rev. Lett.* **94** 032301
[12] PHOBOS Collaboration 2003 *Phys. Rev. Lett.* **91** 052303
[13] Murray M (for BRAHMS Collaboration) 2005 *Proc. Int. Europhysics Conf. on High Energy Physics*
[14] PHOBOS Collaboration 2005 *Phys. Rev. Lett.* **94** 122303
[15] PHOBOS Collaboration 2006 *Preprint* nucl-ex/0511045
[16] BRAHMS Collaboration 2003 *Phys. Rev. Lett.* **90** 102301
[17] Landau L 1953 *Izv. Akad. Nauk. SSSR* **17** 15
[18] Milekhin G A 1958 *Zh. Eksp. Teor. Fiz.* **35** 1185
[19] Carruthers P and Duong-van M 1972 *Phys. Lett.* B **41** 597
[20] Carruthers P and Duong-van M 1973 *Phys. Rev.* D **8** 859
[21] Cooper F and Schonberg E 1973 *Phys. Rev. Lett.* **30** 880
[22] Staszel P (for BRAHMS Collaboration) 2005 *Preprint* nucl-ex/0510061
[23] Fries R J *et al* 2003 *Phys. Rev.* C **68** 044902
[24] Greco V *et al* 2005 *Phys. Rev.* C **71** 041901R
[25] Hwa R C and Yang C B 2004 *Phys. Rev.* C **70** 024905
[26] Vitev I and Gyulassy M 2003 *Nucl. Phys.* A **715** 779c
[27] Pop V T *et al* 2004 *Phys. Rev.* C **70** 064906
[28] PHENIX Collaboration 2003 *Phys. Rev. Lett.* C **91** 172301
[29] Hirano T and Nara Y 2003 *Phys. Rev.* C **68** 064902
[30] Becattini F *et al* 2001 *Phys. Rev.* C **64** 024901
[31] BRAHMS Collaboration 2003 *Phys. Rev. Lett.* **91** 072305
[32] Kopeliovich B Z *et al* 2005 *Phys. Rev.* C **72** 054606
[33] Barnafoldi C *et al* 2005 *Preprint* hep-ph/0511190
[34] BRAHMS Collaboration 2004 *Phys. Rev. Lett.* **93** 242303